

UCSF

UC San Francisco Previously Published Works

Title

Amyloid, tau and metabolic PET correlates of cognition in early and late-onset Alzheimer's disease

Permalink

<https://escholarship.org/uc/item/8rr5863h>

Journal

Brain, 145(12)

ISSN

0006-8950

Authors

Tanner, Jeremy A
Iaccarino, Leonardo
Edwards, Lauren
[et al.](#)

Publication Date

2022-12-19

DOI

10.1093/brain/awac229

Peer reviewed



Amyloid, tau and metabolic PET correlates of cognition in early and late-onset Alzheimer's disease

Jeremy A. Tanner,¹ Leonardo Iaccarino,¹ Lauren Edwards,¹ Breton M. Asken,¹ Maria L. Gorno-Tempini,¹ Joel H. Kramer,¹ Julie Pham,¹ David C. Perry,¹ Katherine Possin,¹ Maura Malpetti,^{1,2} Taylor Mellinger,¹ Bruce L. Miller,¹ Zachary Miller,¹ Nidhi S. Mundada,¹ Howard J. Rosen,¹ David N. Soleimani-Meigooni,¹ Amelia Strom,¹ Renaud La Joie¹ and Gil D. Rabinovici^{1,3,4}

Early-onset (age < 65) Alzheimer's disease is associated with greater non-amnestic cognitive symptoms and neuro-pathological burden than late-onset disease. It is not fully understood whether these groups also differ in the associations between molecular pathology, neurodegeneration and cognitive performance.

We studied amyloid-positive patients with early-onset ($n = 60$, mean age 58 ± 4 , MMSE 21 ± 6 , 58% female) and late-onset ($n = 53$, mean age 74 ± 6 , MMSE 23 ± 5 , 45% female) Alzheimer's disease who underwent neurological evaluation, neuropsychological testing, ¹¹C-Pittsburgh compound B PET (amyloid-PET) and ¹⁸F-flortaucipir PET (tau-PET). ¹⁸F-fluorodeoxyglucose PET (brain glucose metabolism PET) was also available in 74% ($n = 84$) of participants. Composite scores for episodic memory, semantic memory, language, executive function and visuospatial domains were calculated based on cognitively unimpaired controls. Voxel-wise regressions evaluated correlations between PET biomarkers and cognitive scores and early-onset versus late-onset differences were tested with a PET \times Age group interaction. Mediation analyses estimated direct and indirect (¹⁸F-fluorodeoxyglucose mediated) local associations between ¹⁸F-flortaucipir binding and cognitive scores in domain-specific regions of interest.

We found that early-onset patients had higher ¹⁸F-flortaucipir binding in parietal, lateral temporal and lateral frontal cortex; more severe ¹⁸F-fluorodeoxyglucose hypometabolism in the precuneus and angular gyrus; and greater ¹¹C-Pittsburgh compound B binding in occipital regions compared to late-onset patients. In our primary analyses, PET-cognition correlations did not meaningfully differ between age groups. ¹⁸F-flortaucipir and ¹⁸F-fluorodeoxyglucose, but not ¹¹C-Pittsburgh compound B, were significantly associated with cognition in expected domain-specific patterns in both age groups (e.g. left perisylvian/language, frontal/executive, occipital/visuospatial). ¹⁸F-fluorodeoxyglucose mediated the relationship between ¹⁸F-flortaucipir and cognition in both age groups across all domains except episodic memory in late-onset patients. Additional direct effects of ¹⁸F-flortaucipir were observed for executive function in all age groups, language in early-onset Alzheimer's disease and in the total sample and visuospatial function in the total sample.

In conclusion, tau and neurodegeneration, but not amyloid, were similarly associated with cognition in both early and late-onset Alzheimer's disease. Tau had an association with cognition independent of neurodegeneration in language, executive and visuospatial functions in the total sample. Our findings support tau PET as a biomarker that captures both the clinical severity and molecular pathology specific to Alzheimer's disease across the broad spectrum of ages and clinical phenotypes in Alzheimer's disease.

- 1 Memory and Aging Center, Department of Neurology, University of California San Francisco (UCSF), San Francisco, CA 94158, USA
- 2 Department of Clinical Neurosciences, University of Cambridge, Cambridge, UK
- 3 Department of Radiology and Biomedical Imaging, University of California San Francisco (UCSF), San Francisco, CA 94143, USA
- 4 Weill Institute for Neurosciences, University of California San Francisco (UCSF), San Francisco, CA 94158, USA

Correspondence to: Jeremy A. Tanner
 UCSF Memory and Aging Center
 Box 1207, 675 Nelson Rising Lane
 Suite 190, San Francisco, CA 94143, USA
 E-mails: jeremy.tanner@ucsf.edu; jeremy.a.tanner@gmail.com

Keywords: Alzheimer's disease; early-onset; PET; tau; cognition

Abbreviations: CDR = Clinical Dementia Rating; EOAD = early-onset Alzheimer's disease; FDG = ¹⁸F-fluorodeoxyglucose; FTP = ¹⁸F-flortaucipir; LOAD = late-onset Alzheimer's disease; MMSE = Mini-Mental State Examination; PIB = ¹¹C-Pittsburgh compound B; SUVR = standardized uptake value ratio

Introduction

While its prevalence increases exponentially with age, Alzheimer's disease is also a leading cause of early-onset dementia.^{1,2} Early-onset Alzheimer's disease (EOAD), defined in most studies as developing in patients younger than age 65, comprises an estimated 5.5% of total Alzheimer's disease cases.³ The majority (>90%) of EOAD cases are commonly referred to as sporadic because they lack a known pathogenic autosomal dominant mutation, although heritability of the disease is high, as 35–60% patients have at least one affected first-degree relative.^{4–6} EOAD and late-onset Alzheimer's disease (age ≥ 65, LOAD) share the hallmark neuropathological features of fibrillar amyloid-β and hyperphosphorylated tau. However, patients with EOAD have a greater burden of Alzheimer's disease pathology, particularly neurofibrillary tangles, and appear to have fewer age-related co-pathologies (e.g. TDP-43, vascular infarcts) than LOAD.^{7–12} Cognitive symptoms can also differ between age groups in Alzheimer's disease. Patients with EOAD commonly have greater impairment in visuospatial abilities, executive function and language, but relatively less impairment in episodic and semantic memory.^{13–17} EOAD has a more fulminant disease course characterized by delayed diagnosis, faster disease progression and a higher risk of mortality.^{7,18–23} Nevertheless, patients with EOAD have previously been excluded from many studies of Alzheimer's disease due to their age, leaving many questions unanswered regarding whether the underlying pathophysiology and biomarkers differ across the Alzheimer's disease age spectrum.

Recent advances in neuroimaging enable *in vivo* biomarker comparisons between EOAD and LOAD. Aggregated amyloid-β plaques can be visualized and quantified with radiotracers for fibrillar amyloid-β such as ¹¹C-Pittsburgh compound B (PIB).^{24–26} Prior studies comparing amyloid PET ligand binding between age groups have been mixed, where some have shown greater regional binding in EOAD,^{27,28} while others have found no notable differences.^{29–31} Neurofibrillary tangles composed of aggregated hyperphosphorylated tau can also be detected with specific radiotracers such as ¹⁸F-flortaucipir (FTP).^{32–35} Compared to LOAD, patients with EOAD have greater global tau PET binding and higher neocortical relative to medial temporal binding.^{36–41} Finally, brain glucose metabolism can be evaluated with ¹⁸F-fluorodeoxyglucose-PET (FDG-PET), which is a radiolabelled glucose analogue that is used as a biomarker of synaptic dysfunction and neurodegeneration.⁴² Alzheimer's disease

most commonly presents with FDG-PET hypometabolism in precuneus/posterior cingulate and lateral temporo-parietal regions, with patients with EOAD having more severe hypometabolism in these regions and relative sparing of the medial temporal lobe.^{29,43,44}

Previous PET studies have demonstrated that amyloid PET binding patterns have absent-to-weak correlation with clinical phenotypes or cognitive deficits.^{31,36,45,46} In contrast, both the burden and the distribution of tau PET binding correlate with cognitive symptoms in Alzheimer's disease across heterogeneous clinical phenotypes.^{31,36,38,41,47–50} Similar to tau PET, the degree and distribution of FDG-PET hypometabolism in Alzheimer's disease closely aligns with cognitive symptoms and is more closely correlated with FTP-PET than PIB-PET binding.^{28,29,36,38,51}

Considering their clinical and biomarker differences, it is possible that the correlation between cognitive symptoms and *in vivo* molecular pathology and neurodegeneration may vary between EOAD and LOAD.^{36,38,40,48} This may be due to younger patients having greater Alzheimer's disease pathological burden, faster tau accumulation,⁵² stronger tau correlation with future brain atrophy,⁵³ fewer age-related co-pathologies¹² or biological differences in amyloid and tau pathology compared to older patients.^{54,55} Alternatively, it is plausible that the correlation may be stronger in older patients due to less cognitive and brain resilience to Alzheimer's disease pathology.⁵⁶ No prior studies to our knowledge have systematically evaluated this by directly evaluating the effect of age on the relationships between molecular pathology, neurodegeneration and domain-specific cognitive performance in a clinically diverse cohort of patients with symptomatic Alzheimer's disease.

The objective of this study was to compare the correlation between cognitive symptoms and *in vivo* PET biomarkers in EOAD versus LOAD. *A priori*, we hypothesized that the correlation between FTP-PET and cognitive performance would be stronger in EOAD compared to LOAD. We further hypothesized that cognitive performance would not correlate with PIB-PET binding in EOAD or LOAD.

Materials and methods

Participants

Participants were retrospectively selected from the University of California San Francisco (UCSF) Alzheimer's Disease Research Center clinical cohort. All participants underwent a standard

clinical evaluation including comprehensive history, neurological exam, caregiver interview and brain MRI. Consensus diagnosis was provided by a multidisciplinary team. Participants were initially included if they: (i) met NIA-AA criteria for probable Alzheimer's disease dementia⁵⁷ or mild cognitive impairment due to Alzheimer's disease⁵⁸; (ii) had a positive amyloid PIB-PET scan by expert visual read; (iii) underwent FTP-PET; and (iv) had neuropsychological testing within 1 year of their FTP-PET scan, resulting in 127 participants. Participants were then excluded ($n = 14$) if they: (i) met research criteria for an additional dementia type, including traumatic encephalopathy syndrome,⁵⁹ at the time of FTP-PET scan ($n = 11$); (ii) had chronic alcohol abuse within 6 months of neuropsychological testing ($n = 1$); or (iii) had incomplete neuropsychological testing ($n = 1$) or FTP-PET acquisition ($n = 1$). Of participants in the final cohort ($n = 113$), 20 additionally met clinical criteria for posterior cortical atrophy (PCA)⁶⁰ and 22 patients for logopenic variant primary progressive aphasia (lvPPA).⁶¹ FDG-PET was available in 74% ($n = 84$) of participants.

EOAD ($n = 60$) was defined as patients' age < 65 and LOAD ($n = 53$) were those age ≥ 65 at the time of FTP-PET. Chronological age (as opposed to age at symptom onset) at time of FTP-PET scan was used to reduce subjectivity in estimating symptom onset by the patient or caregiver. In supplementary analyses, we included two different cognitively unimpaired healthy control (HC) groups to estimate PET biomarker changes at the group-level. Two HC groups were used due to the limited number of healthy control subjects who had completed all three PET scan modalities. HC Group 1 completed both PIB-PET and FTP-PET ($n = 74$, mean age 67 ± 18 , age range 21–93, 53% female, 17 ± 2 years education). HC Group 2 completed FDG-PET ($n = 78$, mean age 67 ± 15 , age range 22–90, 55% female, 17 ± 2 years education).

Cognitive testing

Methods for neuropsychological testing and composite scores for each cognitive domain have previously been described.^{47,62} Briefly, episodic memory was measured using California Verbal Learning Test—Short Form and Benson Figure delayed recall. Semantic memory was measured using Boston Naming Test—Short Form, Peabody Picture Vocabulary Test—Revised Comprehension and Category Fluency (animals). Language was measured using Curtiss–Yamada Comprehensive Language Evaluation—receptive comprehension subtest, verbal agility and oral repetition. Executive function was measured with digits backward, Letter Fluency ('D' words in 1 min), Design Fluency—condition one, Modified Trail Making Test and Stroop inhibition. Visuospatial functioning was measured by the Benson Figure copy and the Number Location subtest of the Visual Object and Spatial Perception test.

Composite scores from neuropsychological testing were created for each cognitive domain for each participant. Participant neuropsychological testing scores were converted to W -scores adjusted for age using testing scores from a previously described UCSF sample of 564 cognitively unimpaired participants (mean age 67 ± 7 ; mean years of education 17 ± 2).⁴⁷ To generate composite scores for each domain, participant W -scores were averaged for all tests within that domain (tests with multiple components were weighted to serve as one score). When participants had individual tests missing, composite scores were calculated from available individual tests scores within that cognitive domain. Composite scores were available for 111/113 participants in executive function, for 112/113 in episodic memory and visuospatial function and for all participants in semantic memory and language. Higher W -scores were representative of greater cognitive impairment. When adjusting for years of education

in addition to age, W -scores remained highly similar ($\rho \geq 0.94$, $R^2 \geq 0.91$ in all domains) and maintained similar associations with PET standardized uptake value ratio (SUVR) across modalities, and thus education was not included as a covariate in the final models.

To account for clinical severity, we created a combined global cognitive measure (zMMSECDR) that was calculated as the mean of the Z -scores of the Mini-Mental State Examination (MMSE) and Clinical Dementia Rating (CDR) Sum of Boxes within the total patient sample. This aggregated measure was previously developed⁶³ to attempt to balance biases in CDR Sum of Boxes (less sensitive to language impairment)⁶⁴ and MMSE (less sensitive to visuospatial impairment).⁶⁵

Image acquisition and processing

Acquisition protocols for all imaging modalities have previously been described by Iaccarino *et al.*³⁹ and methods are further detailed in the [Supplementary material](#). All participants underwent structural MRI (mean 21 ± 42 days between MRI and neuropsychological tests), PIB-PET (mean 60 ± 73 days between PIB-PET and neuropsychological tests) and FTP-PET (mean 62 ± 76 days between FTP-PET and neuropsychological tests). Eighty-four participants underwent FDG-PET (mean 84 ± 82 days between FDG-PET and neuropsychological tests). MRI scans were performed at UCSF with a high-resolution T_1 magnetization-prepared rapid gradient-echo sequence either on a 3T Siemens Tim Trio ($n = 34$) or Prisma Fit ($n = 79$) scanner with similar acquisition parameters.³⁹ PET scans were acquired at Lawrence Berkeley National Laboratory (LBNL) on a Siemens Biograph 6 Truepoint PET/CT scanner in 3D acquisition mode. Attenuation correction was performed using a low-dose CT/transmission scan acquired prior to PET. PIB-PET, FTP-PET and FDG-PET were all processed to obtain SUVR maps, with PIB-PET at 50–70 min post-injection, FTP-PET at 80–100 min post-injection and FDG-PET at 30–60 min post-injection. Tracer-specific reference regions were selected as cerebellar grey matter for PIB-PET, inferior cerebellar grey matter for FTP-PET and pons for FDG-PET. For summary measures, we calculated a PIB-PET neocortical composite SUVR,⁶⁶ then converted this to Centiloid values using previously described methods.⁶⁷ For FTP-PET, a summary SUVR was calculated for a composite temporal region of interest (metaROI)⁶⁸ and for Braak neuropathological stage regions of interest.^{69,70} In sensitivity analyses to evaluate whether group differences may be due to differences in grey matter volume, we applied three-compartment partial volume corrections to PIB-PET⁷¹ and compared grey matter volumes between age groups. Neuroimaging data were processed using Statistical Parametric Mapping version 12 (SPM12, <https://www.fil.ion.ucl.ac.uk/spm/>) software in MATLAB, 2015.⁷²

Statistical and image analyses

Demographics

Demographic, global biomarker, and cognitive scores were compared between age groups using two-tailed t -tests for continuous and χ^2 for categorical variables and considered significant if $P < 0.05$. Effect size was estimated by calculating Cohen's d for continuous and Cramér's V for categorical variables.

Group-level biomarker comparison

Mean images were generated for each PET imaging modality (i.e. PIB-PET, FTP-PET, FDG-PET) for the total sample and for both EOAD and LOAD groups for visualization. Then, EOAD and LOAD groups

were compared in each imaging modality to each other (without covariates) and to the HC groups (controlling for age) to identify group-level differences. Voxel-wise group comparisons were performed with SPM12 using two-sample t-tests, setting $P < 0.001$, $k > 100$ voxels uncorrected for multiple comparisons as primary statistical threshold. Additionally, only clusters surviving a $P < 0.05$ family-wise error correction at the cluster level were deemed significant. In sensitivity analyses, EOAD versus LOAD group comparisons were repeated adding a covariate for global cortical tracer-specific signal based on FreeSurfer defined cortical regions of interest, using the same threshold for significance.

Clinical-functional correlations

Next, we performed voxel-wise regressions to evaluate the correlation between each imaging modality and each cognitive domain age-corrected W -score in the total sample and then within each age group. An interaction term was included in a separate model to directly compare voxel-wise correlations between age groups. Primary analyses were conducted without covariates. Disease severity covariates were not included due to high collinearity between composite cognitive domains and global cognitive measures (e.g. MMSE, zMMSECDR). We applied the same statistical thresholds and corrections described above for group-level analyses. Results were visualized using BrainNet Viewer software with an interpolated

mapping algorithm.⁷³ As a quality control measure for possible outliers or spurious effects, we created and evaluated scatterplots using R (version 4.0) and package ggplot2 for each individual model.^{74,75} To do so, we isolated the significant clusters from each total sample voxel-wise model, then extracted the average SUVR values for each participant for the given modality. These values were then plotted with the respective cognitive scores across age groups to evaluate their associations.

Sensitivity analyses included: (i) voxel-wise analyses repeated after adding a disease severity covariate (i.e. zMMSECDR); (ii) voxel-wise analyses repeated after excluding cases meeting diagnostic criteria for atypical Alzheimer's disease variants (i.e. PCA or lvPPA); (iii) voxel-wise analyses repeated after adding a covariate for global cortical tracer-specific signal to account for global pathological burden; and (iv) using alternative age group thresholds (age 60 and age 70) to divide groups and replotting the correlation between cognitive performance and mean PET SUVR to explore for age threshold effects.

Region of interest-level mediation analyses

We then performed causal mediation analyses and complementary multiple regression analyses to further explore the intermediary role of hypometabolism in the local relationship between tau and

Table 1 Group characteristics^a

Variable	Total (n = 113)	EOAD (n = 60)	LOAD (n = 53)	P-value	Effect size ^b
Age at PET scan (years), mean (SD)	65.5 (9.3)	58.1 (3.9)	73.9 (5.9)	<0.001	3.20
Female sex, % (n)	52% (59)	58% (35)	45% (24)	0.17	0.13
Race and ethnicity, % (n)				0.16	0.24
Asian or Pacific Islander	4% (4)	3% (2)	4% (2)		
Black or African American	1% (1)	2% (1)	0		
Hispanic or Latino	2% (2)	3% (2)	0		
White	90% (102)	85% (51)	96% (51)		
Declined to state	4% (4)	7% (4)	0		
Education (years), mean (SD)	16.8 (2.7)	16.7 (3.0)	16.9 (2.4)	0.66	0.08
Clinical diagnosis, % (n)				0.15	0.22
Mild cognitive impairment	18% (20)	12% (7)	25% (13)		
Alzheimer's disease dementia	45% (51)	43% (26)	47% (25)		
Posterior cortical atrophy	18% (20)	23% (14)	11% (6)		
Logopenic variant primary progressive aphasia	19% (22)	22% (13)	17% (9)		
Amnesic presentation, % (n)	56% (63)	47% (28)	66% (35)	0.04	0.19
ApoE4 ϵ 4 allele, % (n)				0.88	0.05
None	43% (40)	45% (23)	41% (17)		
Heterozygous	43% (40)	41% (21)	46% (19)		
Homozygous	13% (12)	14% (7)	12% (5)		
PIB-PET Centiloid, mean (SD)	92 (34)	98 (27)	85 (39)	0.03	0.41
FTP-PET temporal metaROI SUVR, mean (SD)	2.0 (0.5)	2.2 (0.5)	1.9 (0.5)	<0.001	0.66
MMSE, mean (SD)	22.0 (5.7)	20.9 (6.2)	23.3 (4.8)	0.03	0.42
CDR \leq 0.5, % (n)	58% (66)	53% (32)	64% (34)	0.24	0.11
CDR Sum of Boxes, mean (SD)	3.9 (2.1)	4.0 (2.1)	3.8 (2.2)	0.51	0.12
CD \leq 0.5 in lvPPA/PCA, % (n)	62% (26)	67% (18)	53% (8)	0.39	0.13
Z-score MMSECDRSum, mean (SD) ^{c,d}	0.0 (1.8)	0.2 (1.9)	-0.3 (1.7)	0.11	0.30
Episodic memory, W-score mean (SD) ^d	2.6 (1.3)	2.8 (1.4)	2.4 (1.2)	0.14	0.28
Semantic memory, W-score mean (SD) ^d	2.0 (1.9)	2.0 (1.8)	2.1 (2.1)	0.78	0.05
Language, W-score mean (SD) ^d	1.9 (2.3)	2.4 (2.3)	1.4 (2.2)	0.01	0.47
Executive function, W-score mean (SD) ^d	1.9 (1.2)	2.3 (1.1)	1.4 (1.1)	<0.001	0.78
Visuospatial, W-score mean (SD) ^d	2.5 (3.6)	3.7 (3.9)	1.2 (2.8)	<0.001	0.75

Bold font indicates significant differences between EOAD and LOAD groups.

^aPearson χ^2 and two-tailed t-tests were used to assess baseline group differences.

^bEffect size was measured using Cramér's V and Cohen's d .

^cMean of the Z-score of the MMSE and CDR Sum of Boxes.

^dHigher scores indicate greater impairment.

domain-specific cognitive performance in regions where cognition was related to both FTP-PET and FDG-PET. In particular, we aimed to use *in vivo* PET biomarkers to evaluate whether neurofibrillary tangles have an association with cognitive performance independent of neurodegeneration, or if the association is solely mediated by neurodegeneration. We performed this for each cognitive domain to explore this question across multiple known brain-behaviour relationships. For these analyses, average FTP-PET and FDG-PET SUVRs were extracted for each participant from the overlapping clusters from the respective total group correlation models for each cognitive domain.

Causal mediation analyses were performed for the total group and then stratified according to age group with R (version 4.0, mediation package).⁷⁶ This determined (i) the average direct effect of FTP-PET SUVR on cognitive performance; and (ii) the average

causal mediation effect, reflecting the indirect effect of FTP-PET SUVR on cognitive performance that is mediated by FDG-PET SUVR. All measurements were estimated using non-parametric bootstrapping (1000 simulations, $P < 0.05$). In exploratory analyses, we evaluated whether there was a difference between age groups by including age group as a moderator in the mediation between FTP-PET, FDG-PET and domain-specific cognitive performance. We ran two-group structural equation modelling analyses (lavaan R package) to directly compare the estimation of each mediation parameter between groups using the Wald test and the likelihood ratio test.

As complementary analyses, we performed partial correlation and multiple linear regressions in the total sample and then in EOAD and LOAD groups. We used domain-specific cognitive performance as the dependent variable and mean FTP-PET and

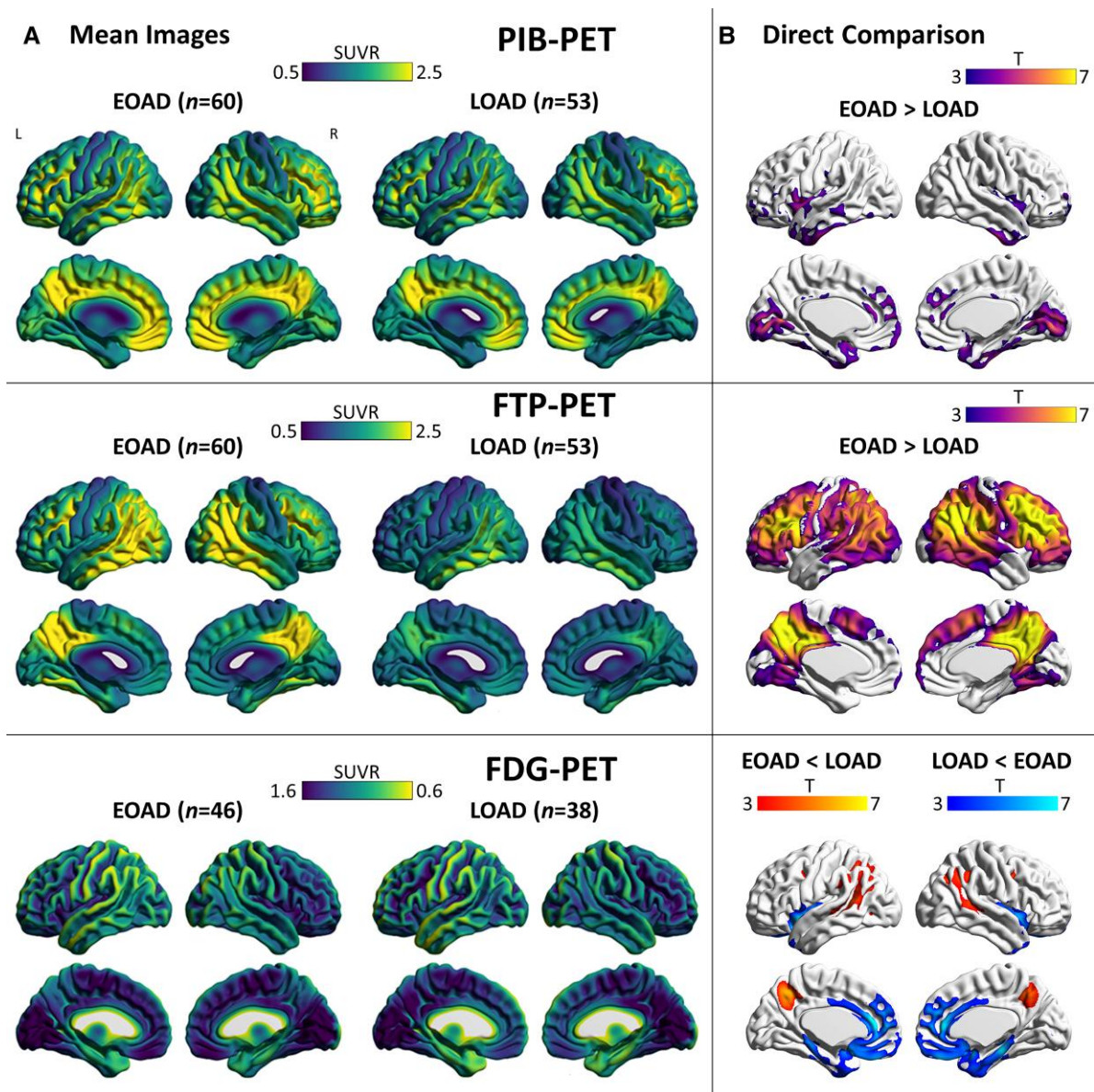


Figure 1 Mean images and group comparisons of biomarkers. (A) Mean interpolated surface projections of average SUVR maps are displayed for EOAD and LOAD subgroups for PIB-PET, FTP-PET and FDG-PET. (B) Voxel-wise comparisons between groups, with significant differences presented at a peak-level threshold of $P < 0.001$ uncorrected, cluster-level family-wise error corrected $P < 0.05$.

FDG-PET SUVR as independent variables. We then performed a Chow test to compare regressions between age groups.

Informed consent

Written informed consent was obtained from all patients or their surrogates. The study was approved by the University of California (San Francisco and Berkeley) and LBNL institutional review boards for human research.

Data availability

To promote data transparency, data are available upon request (<https://memory.ucsf.edu/research-trials/professional/open-science>).

Results

Participants

Group characteristics including demographic, clinical, PET biomarker summary measures and cognitive composite scores are reported

in Table 1 (additional details listed in Supplementary Table 1). There were no significant differences between Alzheimer's disease participants and HC groups in age, sex or years of education [HC Group 1: $t(185) = -0.90$, $P = 0.37$; $\chi^2(1) = 0.004$, $P = 0.95$; $t(184) = -0.96$, $P = 0.34$, respectively; HC Group 2: $t(160) = -0.76$, $P = 0.44$; $\chi^2(1) = 0.43$, $P = 0.51$; $t(157) = 0.08$, $P = 0.94$, respectively].

Participants with EOAD were 15.8 years younger on average than participants with LOAD, and this was similar when using age of symptom onset to divide groups (14.9 years). They more frequently presented with non-amnesic symptoms (i.e. visuospatial, language, executive function) than participants with LOAD (53% and 34%, respectively). There were no significant differences in Alzheimer's disease clinical syndrome subtypes between age groups. Patients with lvPPA accounted for 22% of EOAD and 17% of LOAD participants, and PCA was present in 23% of EOAD and 11% of LOAD participants. EOAD participants had significantly greater PIB-PET signal (with and without partial volume correction) and greater FTP-PET binding in temporal metaROI, Braak III&IV and Braak V&VI regions. Additionally, EOAD participants had lower MMSE scores, but there was no significant difference between groups in CDR Sum of Boxes

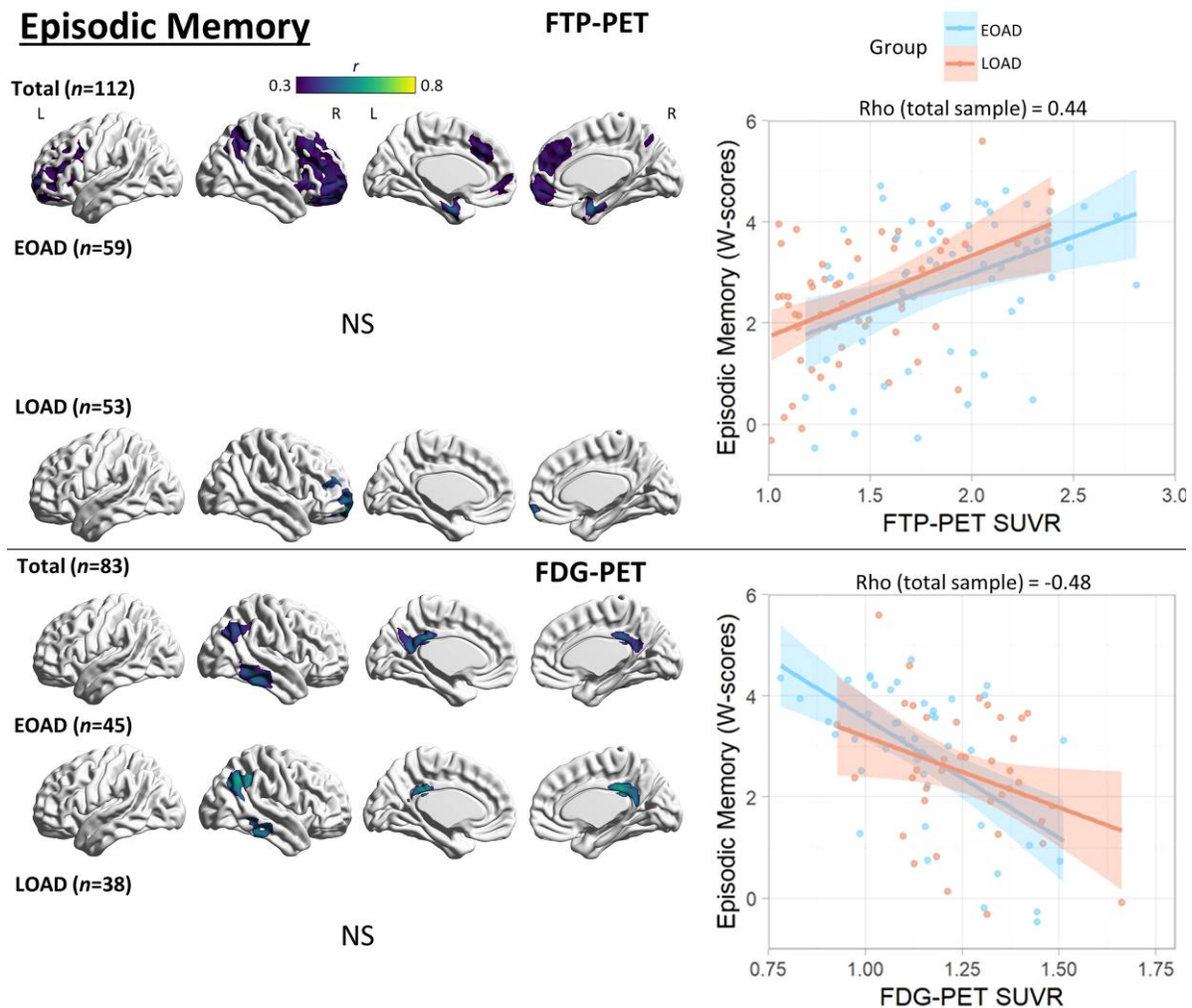


Figure 2 Voxel-wise correlation between episodic memory and PET neuroimaging. Voxel-wise regression analyses showing correlation between episodic memory W-scores and each imaging modality for the total sample and for each age group. Pearson correlation coefficients (left) are shown for voxels significant at a peak-level threshold of $P < 0.001$ uncorrected, cluster-level family-wise error corrected $P < 0.05$. Scatterplots (right) were obtained by extracting average SUVR values from significant clusters for the total sample and plotted separately by age group. Higher W-scores indicate more severe impairment. NS = not significant.

or zMMSECDR. On cognitive testing, participants with EOAD performed significantly worse in language, executive function and visuospatial but not in episodic or semantic memory domains.

PET imaging biomarker abnormalities

Mean images for each imaging modality for the total sample (Supplementary Fig. 1) and each age group (Fig. 1A) are displayed. Overall, PIB-PET, FTP-PET and FDG-PET hypometabolism aligned with the expected Alzheimer's disease signature regional patterns in all groups.

Direct voxel-wise comparisons between patient groups and controls are shown, respectively, in Fig. 1B and Supplementary Fig. 2. Patients with EOAD had increased PIB-PET SUVR compared to those with LOAD in the medial occipital lobe and in small clusters in the medial frontal and anterior temporal cortices, although only occipital findings remained significant at more restrictive statistical thresholds (primary $P < 0.05$ family-wise error corrected; data not shown). For FTP-PET, participants with EOAD had greater binding compared to those with LOAD in Alzheimer's disease signature regions (medial parietal, lateral temporo-parietal/frontal cortices),

but there were no significant group differences in the inferior lateral and medial temporal cortices. There were no regions where LOAD had significantly greater PIB-PET or FTP-PET SUVR than EOAD. For FDG-PET, participants with EOAD had small clusters of greater hypometabolism in the precuneus and angular gyrus compared to those with LOAD. Participants with LOAD had greater hypometabolism in the medial temporal lobe and in medial frontal regions. In sensitivity analysis, EOAD versus LOAD group comparisons were repeated controlling for global cortical signal (Supplementary Fig. 3). Results were similar, except patients with LOAD had greater FTP-PET SUVR in the anterior and inferomedial temporal cortex and in the medial frontal cortex compared to those with EOAD.

Voxel-wise correlation between cognition and neuroimaging: comparison between age groups

Voxel-wise regressions were performed between each imaging modality and each cognitive domain, and an interaction term was included to compare voxel-wise correlations between age groups. There were no significant interactions between age group and PIB-PET SUVR. There were no significant Age group \times FTP-PET

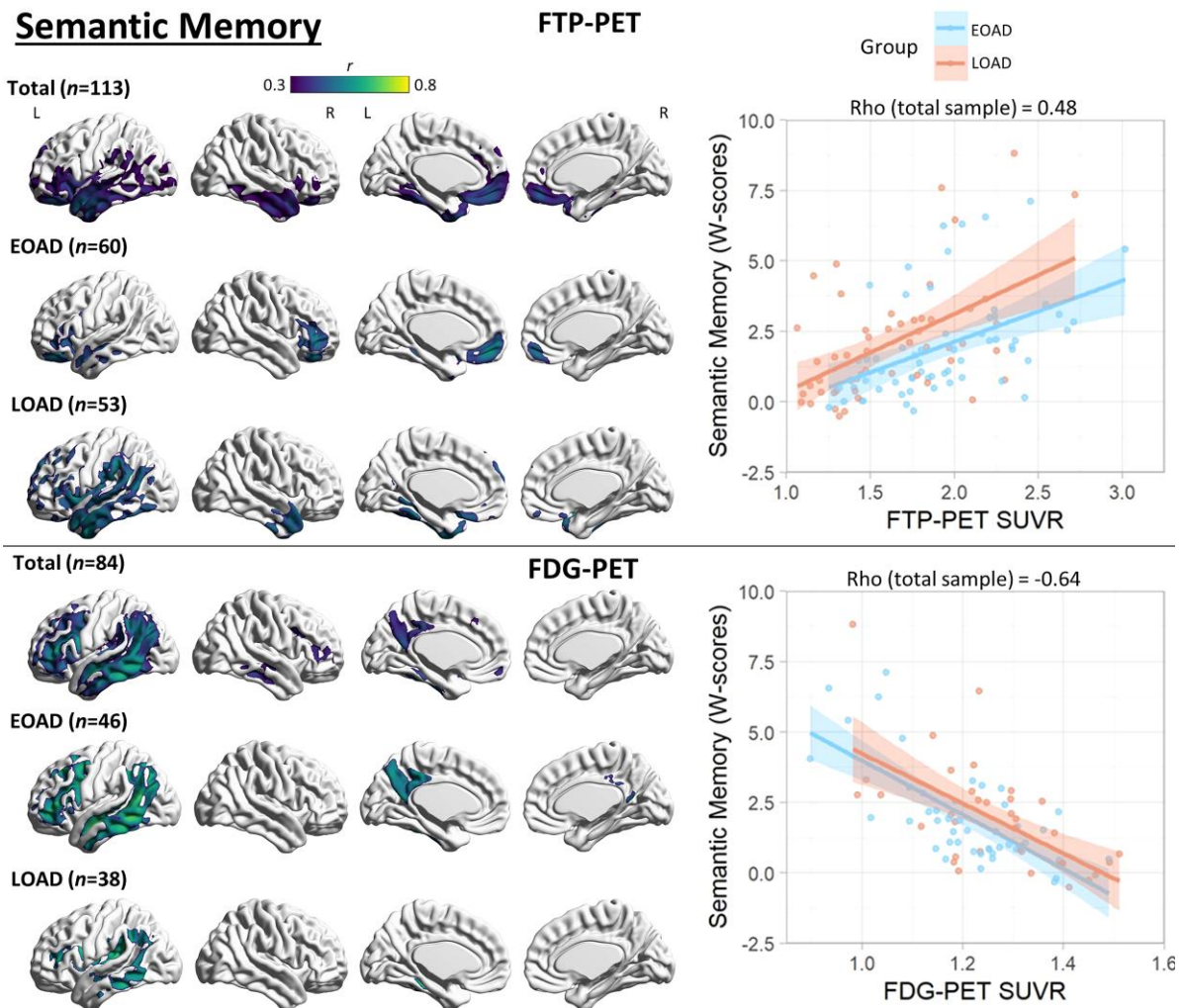


Figure 3 Voxel-wise correlation between semantic memory and PET neuroimaging. Voxel-wise regression analyses showing correlation between semantic memory W-scores and each imaging modality for the total sample and for each age group. Pearson correlation coefficients (left) are shown for voxels significant at a peak-level threshold of $P < 0.001$ uncorrected, cluster-level family-wise error corrected $P < 0.05$. Scatterplots (right) were obtained by extracting average SUVR values from significant clusters for the total sample, and plotted separately by age group. Higher W-scores indicate more severe impairment.

interactions for episodic memory, semantic memory, language or executive function performance. The only significant Age group \times FTP-PET interaction was for visuospatial performance, where FTP-PET SUVR in the right cuneus showed a stronger correlation with visuospatial impairment in the LOAD group compared to the EOAD group (Supplementary Fig. 4). There were no significant interactions between age group and FDG-PET SUVR.

Voxel-wise correlation between cognition and neuroimaging: within age groups

The results of voxel-wise regressions between each cognitive domain and each neuroimaging modality for the total sample and both age groups are displayed in Figs 2–6.

Episodic memory

For PIB-PET, there was no significant association with episodic memory performance. In the total sample, FTP-PET SUVR correlation with episodic memory peaked in the bilateral medial temporal lobes, with a weaker but significant association observed in bilateral lateral and medial frontal and right lateral parietal cortices. Within

age groups, no significant associations were observed in EOAD. Right prefrontal FTP-PET SUVR correlated with episodic memory in LOAD. In *post hoc* analyses using a more liberal statistical threshold (primary $P < 0.001$ uncorrected) to explore for trends, FTP-PET SUVR in the bilateral medial temporal lobe in both age groups and bilateral frontal cortex in LOAD correlated with episodic memory performance (Supplementary Fig. 5). FDG-PET hypometabolism correlated with episodic memory in the right inferior temporal cortex, right angular gyrus and bilateral posterior cingulate cortices in both the total sample and in the EOAD group. There was no significant correlation in the LOAD group. See Fig. 2 for details.

Semantic memory

There was no significant association between PIB-PET and semantic memory performance. FTP-PET SUVR significantly correlated with semantic memory in the total sample in the left greater than right anterior temporal (strongest), inferior frontal (medial and lateral) and fusiform gyri. In EOAD, the correlation was significant in the bilateral ventral frontal and left anterior temporal regions. In LOAD, the correlation was significant in bilateral anterior temporal and left-

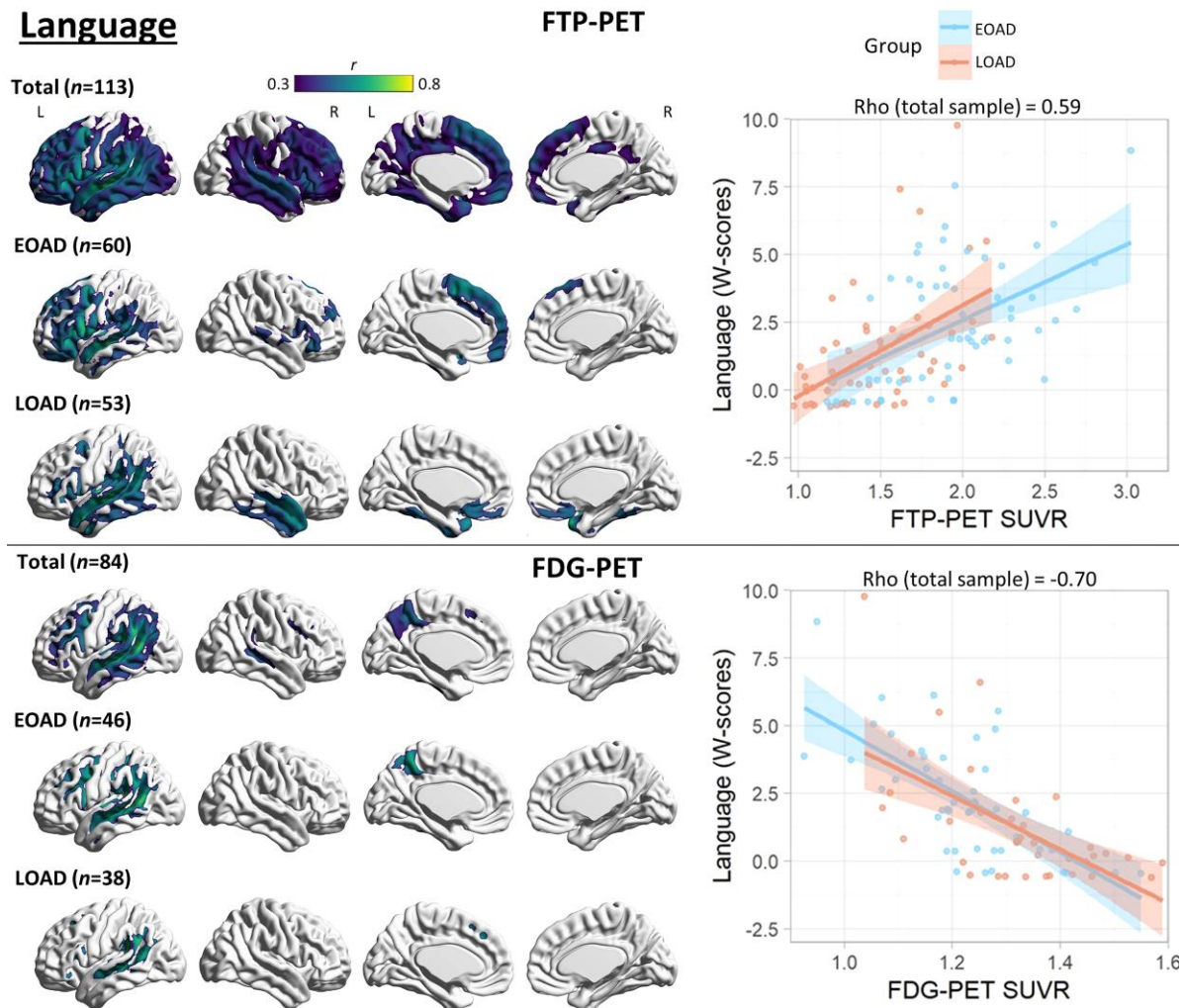


Figure 4 Voxel-wise correlation between language and PET neuroimaging. Voxel-wise regression analyses showing correlation between language W-scores and each imaging modality for the total sample and for each age group. Pearson correlation coefficients (left) are shown for voxels significant at a peak-level threshold of $P < 0.001$ uncorrected, cluster-level family-wise error corrected $P < 0.05$. Scatterplots (right) were obtained by extracting average SUVR values from significant clusters for the total sample and plotted separately by age group. Higher W-scores indicate more severe impairment.

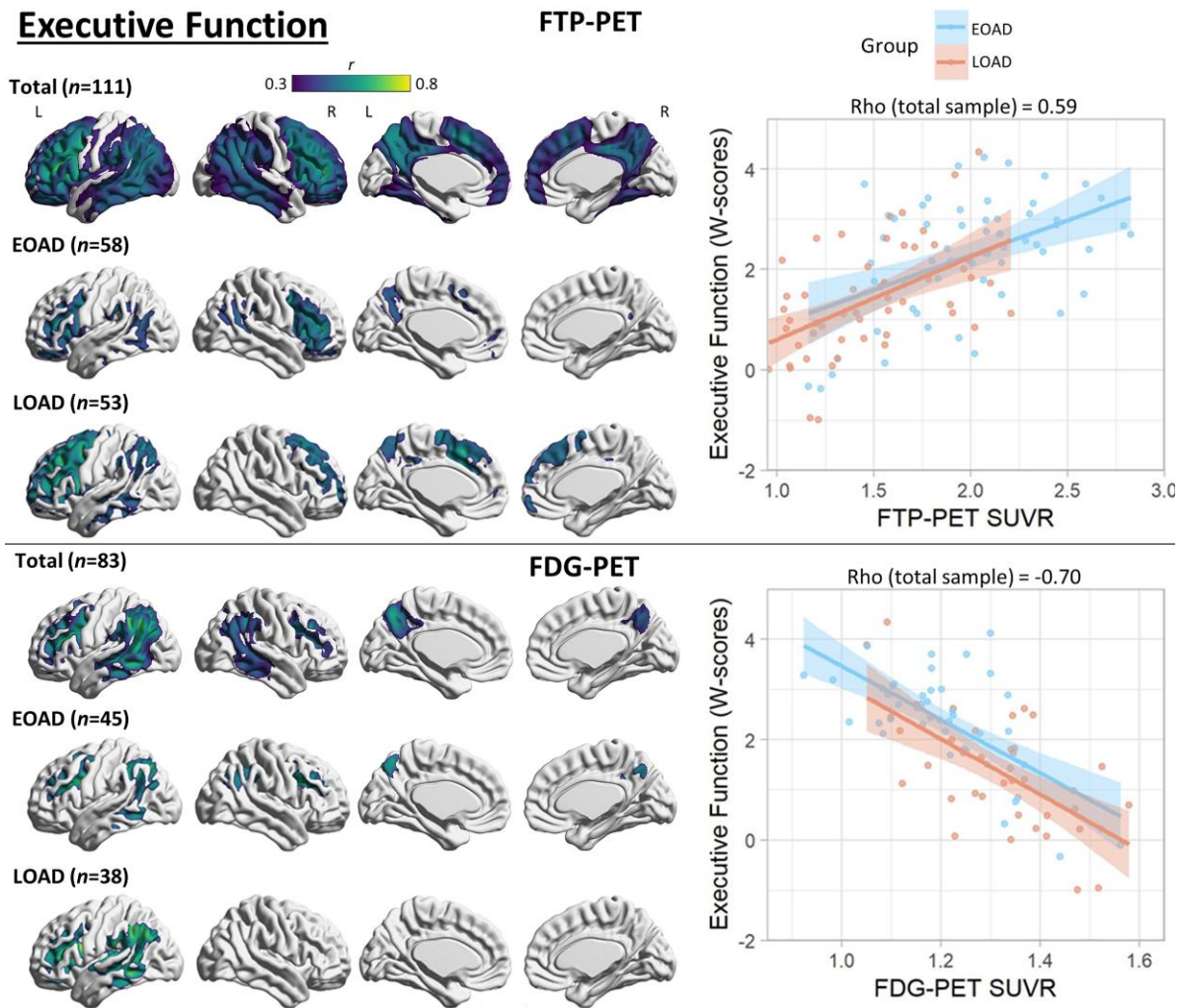


Figure 5 Voxel-wise correlation between executive function and PET neuroimaging. Voxel-wise regression analyses showing correlation between executive function W-scores and each imaging modality for the total sample and for each age group. Pearson correlation coefficients (left) are shown for voxels significant at a peak-level threshold of $P < 0.001$ uncorrected, cluster-level family-wise error corrected $P < 0.05$. Scatterplots (right) were obtained by extracting average SUVR values from significant clusters for the total sample, and plotted separately by age group. Higher W-scores indicate more severe impairment.

predominant perisylvian regions. Correlations with FDG-PET hypometabolism were more widespread and included the left inferior/middle lateral temporal, supramarginal/angular, precuneus/posterior cingulate and lateral frontal cortices in the total sample and in EOAD. In LOAD, the correlation was restricted to the left temporo-parietal region. See Fig. 3 for details.

Language

There was no significant association between language performance and PIB-PET. FTP-PET SUVR correlation with language performance in the total sample peaked in the left > right perisylvian regions with extension throughout the temporal, parietal and frontal cortex. Both age groups had a similar, albeit more spatially restricted, correlation observed mostly in the left perisylvian regions involving the left temporal cortex. Additionally, language was correlated with left frontal binding in EOAD and right temporal binding in LOAD. FDG-PET hypometabolism was more restricted to the left posterior perisylvian regions involving the temporo-parietal cortex in all groups, as well as the left lateral frontal and precuneus in the total sample and EOAD group. See Fig. 4 for details.

Executive function

In the total sample, PIB-PET binding in a small cluster in the right inferior temporal lobe had a weak correlation with executive function scores (Supplementary Fig. 6). In EOAD, PIB-PET binding showed significant associations with worse executive functioning in scattered foci, most prominent in the right orbitofrontal cortex, whereas there was no significant association in LOAD. In the total sample, worse executive function performance was correlated with FTP-PET binding in the bilateral frontal (most prominent left prefrontal cortex), lateral temporal, lateral parietal and medial parietal cortices. There was a similar predominant frontal correlation in both EOAD and LOAD. FDG-PET had a similar, more restricted, correlation with executive function that peaked in the left temporo-parietal cortex. See Fig. 5 for details.

Visuospatial function

PIB-PET was only associated with visuospatial function in the total sample in punctate ventral temporal foci (Supplementary Fig. 6). Visuospatial function was associated with FTP-PET binding in

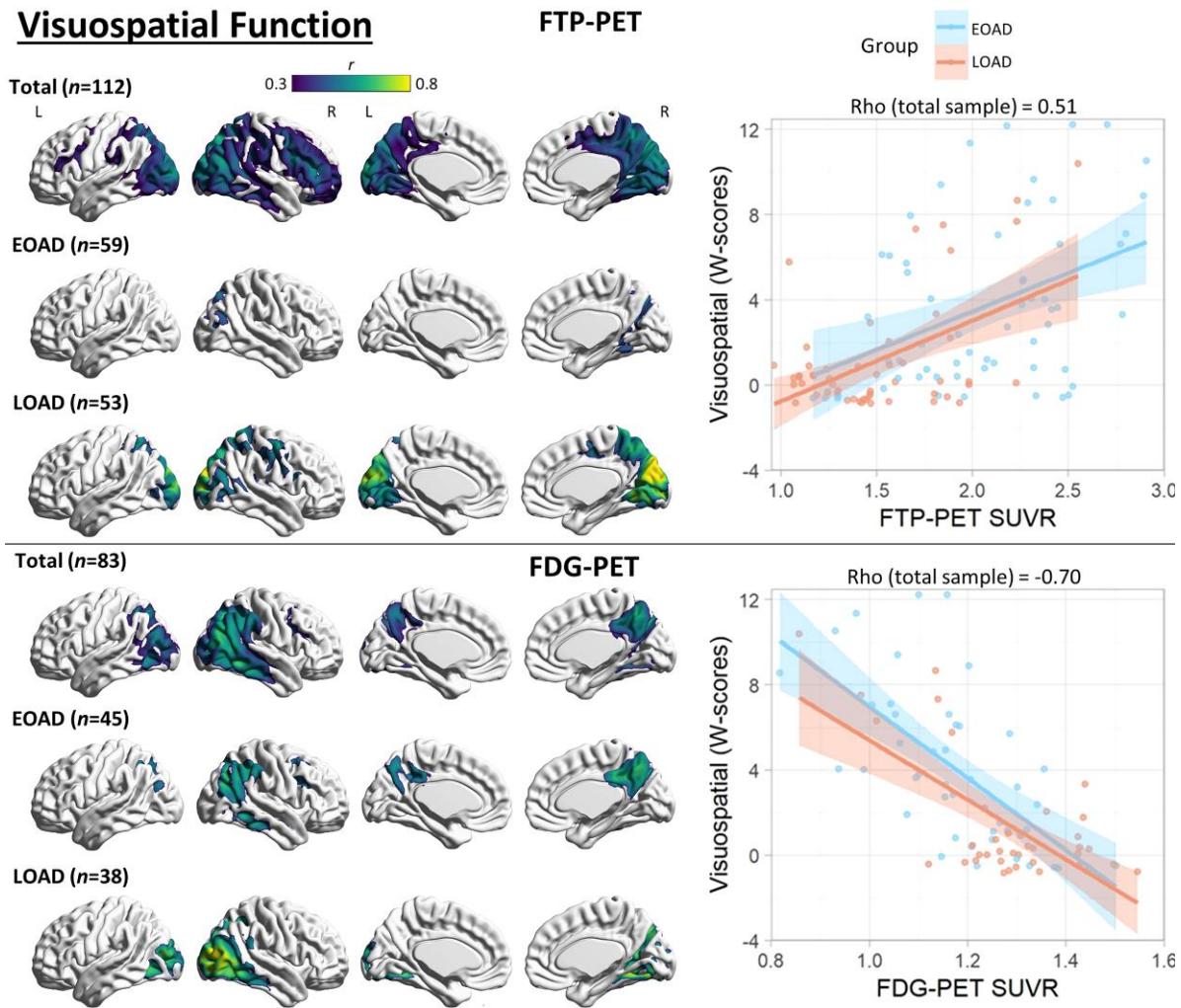


Figure 6 Voxel-wise correlation between visuospatial function and PET neuroimaging. Voxel-wise regression analyses showing correlation between visuospatial function W-scores and each imaging modality for the total sample and for each age group. Pearson correlation coefficients (left) are shown for voxels significant at a peak-level threshold of $P < 0.001$ uncorrected, cluster-level family-wise error corrected $P < 0.05$. Scatterplots (right) were obtained by extracting average SUVR values from significant clusters for the total sample, and plotted separately by age group. Higher W-scores indicate more severe impairment.

the right greater than left dorsolateral prefrontal, posterior parietal and occipital (cuneus most prominent) regions in the total sample and in all age groups, with EOAD showing the most restricted pattern. Visuospatial function was associated with FDG-PET hypometabolism in a similar topography as FTP-PET in the total sample. FDG-PET was more restricted than FTP-PET in the total and LOAD groups, but more extensive in EOAD. See Fig. 6 for details.

Sensitivity analyses

We observed highly similar PET–cognition correlations (albeit with more restricted topography) when including zMMSECDR, a measure of overall clinical severity, as a covariate. This was expected due to the high collinearity between zMMSECDR and the individual cognitive domain scores (Spearman $\rho \geq 0.44$, $P < 0.001$ for all domains). Similar to the primary analyses, the only significant Age group \times PET interaction was for visuospatial performance where the association between FTP-PET SUVR in the right cuneus and visuospatial impairment was stronger in the LOAD group compared to the EOAD group.

Highly similar findings were observed after excluding patients with PCA and lvPPA to test whether the clinical heterogeneity in our cohort was influencing the results (Supplementary Fig. 7). Participants with EOAD tended to have stronger correlations and more widespread regions of significance after excluding these non-amnesic presentations, while participants with LOAD had a more restricted topographical distribution. Significant Age group \times FTP-PET interactions were found for semantic memory where the association between FTP-PET binding in the right greater than left inferior frontal and orbitofrontal cortex and impairment was stronger in EOAD. Significant Age group \times FDG-PET interactions were found for visuospatial function where the association between hypometabolism in the right occipital cortex and impairment was stronger in LOAD. Significant interactions were otherwise inconsistent with primary or other sensitivity analyses.

When co-varying for tracer-specific global cortical signal, we observed similar but notably more restricted PET–cognition correlations (Supplementary Fig. 8). This was also anticipated as global PET SUVR measures were highly collinear with domain-specific regional binding (FTP-PET SUVR: $\rho \geq 0.91$, $P < 0.001$ for all domains; FDG-PET SUVR: $\rho \geq 0.68$, $P < 0.001$ for all domains), which limited

Table 2 Mediation analyses for FTP-PET, FDG-PET (mediator) and domain-specific cognitive performance

	Average causal mediation effect			Average direct effect			Total effect			Proportion mediated		
	Estimate (95% CI)	P-value	Corrected P-value ^a	Estimate (95% CI)	P-value	Corrected P-value	Estimate (95% CI)	P-value	Corrected P-value	Estimate (95% CI)	P-value	Corrected P-value
Total (n = 84)												
Episodic memory	0.28 (0.06–0.56)	0.01	0.02	0.35 (–0.06–0.73)	0.11	0.12	0.63 (0.32–0.94)	<0.001	<0.001	0.45 (0.09–1.17)	0.01	0.02
Semantic memory	1.09 (0.57–1.71)	<0.001	<0.001	0.42 (–0.18–0.99)	0.20	0.22	1.50 (0.88–2.16)	<0.001	<0.001	0.72 (0.42–1.17)	<0.001	<0.001
Language	1.06 (0.60–1.65)	<0.001	<0.001	0.92 (0.23–1.55)	<0.01	0.01	1.98 (1.38–2.63)	<0.001	<0.001	0.54 (0.32–0.86)	<0.001	<0.001
Executive function	0.51 (0.31–0.75)	<0.001	<0.001	0.68 (0.35–1.00)	<0.001	<0.001	1.20 (0.88–1.51)	<0.001	<0.001	0.43 (0.27–0.66)	<0.001	<0.001
Visuospatial	1.64 (1.06–2.34)	<0.001	<0.001	1.26 (0.21–2.35)	0.02	0.02	2.90 (1.89–3.85)	<0.001	<0.001	0.57 (0.34–0.90)	<0.001	<0.001
EOAD (n = 46)												
Episodic memory	0.45 (0.09–0.82)	<0.01	<0.01	0.32 (–0.20–0.89)	0.24	0.26	0.77 (0.15–1.33)	<0.01	0.01	0.59 (0.16–1.89)	<0.01	0.01
Semantic memory	0.95 (0.37–1.60)	<0.001	<0.001	0.77 (0.03–1.50)	0.046	0.056	1.72 (0.94–2.45)	<0.001	<0.001	0.55 (0.24–0.97)	<0.001	<0.001
Language	0.97 (0.27–1.71)	0.01	0.02	1.12 (0.21–1.89)	0.02	0.02	2.09 (1.06–3.02)	<0.001	<0.001	0.47 (0.15–0.86)	0.01	0.02
Executive function	0.40 (0.03–0.78)	0.03	0.04	0.58 (0.11–1.04)	0.02	0.03	0.98 (0.35–1.52)	<0.01	<0.01	0.41 (0.07–0.80)	0.03	0.04
Visuospatial	1.62 (0.69–2.69)	<0.001	<0.001	0.93 (–0.80–2.54)	0.28	0.29	2.55 (0.96–3.90)	<0.01	<0.01	0.64 (0.25–1.63)	<0.01	<0.01
LOAD (n = 38)												
Episodic memory	0.02 (–0.29–0.40)	0.90	0.90	0.64 (–0.13–1.36)	0.09	0.10	0.67 (–0.03–1.31)	0.06	0.07	0.03 (–0.83–1.39)	0.90	0.90
Semantic memory	1.41 (0.38–2.68)	<0.001	<0.001	0.65 (–0.71–2.01)	0.37	0.38	2.06 (0.84–3.37)	<0.001	<0.001	0.68 (0.20–1.58)	<0.001	<0.001
Language	1.17 (0.26–2.57)	<0.01	<0.01	1.32 (–0.02–2.65)	0.06	0.07	2.49 (1.07–4.03)	<0.001	<0.001	0.47 (0.12–1.02)	<0.01	<0.01
Executive function	0.54 (0.14–1.09)	<0.01	<0.01	0.85 (0.16–1.50)	0.02	0.03	1.39 (0.67–2.10)	<0.001	<0.001	0.39 (0.13–0.86)	<0.01	<0.01
Visuospatial	1.56 (0.21–2.92)	0.01	0.02	1.54 (–0.32–3.52)	0.10	0.11	3.10 (0.47–5.22)	0.02	0.03	0.50 (0.11–1.12)	0.03	0.04

In this model, FTP-PET is the independent variable, FDG-PET is the mediator, cognitive domain scores are the dependent variables. Bold font indicates significant differences between EOAD and LOAD groups.
^aP-values with false discovery rate correction for multiple comparisons.

our interpretation of results. Similar to interaction analyses above, significant Age group \times FTP-PET interactions were found for semantic memory where the association between FTP-PET binding in the right inferior frontal cortex and impairment was stronger in EOAD, and for visuospatial function where the association between FTP-PET binding in the right cuneus and impairment was stronger in LOAD. Significant interactions were otherwise inconsistent with primary or other sensitivity analyses.

When using alternative age thresholds to divide age groups (ages 60 and 70), scatterplots displaying correlation between cognitive performance and PET SUVR appeared highly similar to results using the age 65 threshold, suggesting against age threshold effects.

Mediation analyses

Regions of interest used in mediation analyses are displayed in [Supplementary Fig. 9](#). In the total sample and in each age group, FDG-PET significantly mediated the association between FTP-PET and cognitive performance in all cognitive domains except episodic memory in LOAD ([Table 2](#)). In the total sample ($n = 84$), FTP-PET also had a significant direct (i.e. non-FDG-mediated) association with language, executive function and visuospatial performance. In EOAD ($n = 46$), FTP-PET had a significant direct association with language and executive function. In LOAD ($n = 38$), FTP-PET only had a significant direct association with executive function.

Further exploratory analyses to evaluate whether age group moderates the mediation of tau on cognition are displayed in [Supplementary Table 2](#). Overall, there were no meaningful differences identified between age groups in the extent to which FDG-PET mediated the correlation between FTP-PET and domain-specific cognitive performance, although the analyses were underpowered to detect group differences.

In complementary analyses, partial correlations showed that after accounting for FDG-PET SUVR, FTP-PET SUVR remained significantly associated with language, executive function and visuospatial performance in the total sample; language and executive function in EOAD; and executive function and visuospatial performance in LOAD ([Supplementary Fig. 10](#)). Using the Chow test to compare regressions, we observed no significant differences between age groups in all domains (episodic memory: $F = 2.14$, $P = 0.10$; semantic memory: $F = 1.31$, $P = 0.31$; language: $F = 0.70$, $P = 0.55$; executive function: $F = 0.16$, $P = 0.93$; visuospatial: $F = 0.26$, $P = 0.85$).

Discussion

In this study, we assessed the strength and localization of the correlation between *in vivo* PET-based molecular pathology, neurodegeneration, and cognitive performance in EOAD compared to LOAD. We found that the magnitude and topography of each PET–cognition correlation were similar in EOAD and LOAD groups. Overall, tau and neurodegeneration, but not amyloid, correlated with cognitive performance in regions localizing with established brain–behaviour relationships. Neurodegeneration, as measured by FDG-PET, significantly mediated the association between tau and cognition in both age groups. Tau also had an association with cognition in multiple cognitive domains independent of neurodegeneration in the total sample. These results provide insight to the molecular pathology underlying domain-specific cognitive performance across the Alzheimer’s disease age spectrum. Our findings further support the link between tau and cognition, and the potential of tau PET as a biomarker that captures molecular pathology specific to Alzheimer’s

disease and correlates with cognitive performance across the broad range of ages in which patients may develop Alzheimer’s disease.

In keeping with prior studies, we found that participants with EOAD more commonly presented with non-amnesic symptoms and had worse performance in language, visuospatial, and executive function domains compared to those with LOAD.^{13–17} Participants with EOAD had higher levels of tau, amyloid and hypometabolism relative to age-matched controls compared to those with LOAD. Medial temporal lobe regions, however, showed no difference in tau across age groups. Greater cortical relative to medial temporal tau in EOAD compared to LOAD converges with prior neuropathological^{7,8,77} and PET evidence.^{36–38,40,41} This is consistent with more frequent non-amnesic phenotypes in the EOAD group.^{40,77} Additionally, aligning with some of the previous literature,^{27,28} there was a higher burden of amyloid in patients with EOAD compared to LOAD. The direct age-related differences appear notably stronger for tau than for amyloid.

We hypothesized that tau, but not amyloid, would have a stronger correlation with cognitive performance in younger patients. Amyloid did not appear to have a meaningful association with cognitive performance in either age group or in the total sample. This supports prior observations that, in symptomatic disease stages, amyloid has absent-to-weak cross-sectional correlations with cognition in neuroimaging^{47,78,79} and neuropathology^{80,81} studies. Instead, growing evidence suggests that early amyloid accumulation plays a primary role in facilitating tau accumulation and spread, which better correlates with cognition.^{30,52,81,82} The primary mechanisms by which amyloid-lowering agents may impact cognition is therefore by slowing the spread of tau, and indeed the clinical benefit of amyloid lowering may depend on the extent of tau spread prior to initiating treatment.⁸³ It is also possible that amyloid oligomers, considered the most toxic form but not captured in PET imaging, are better correlated with cognitive symptoms in Alzheimer’s disease.^{84–87}

The burden and distribution of tau was significantly associated with worse cognitive performance in each domain in the total sample. We observed significant correlations between tau and cognitive symptoms in alignment with known brain–behaviour relationships. Episodic memory localized with tau predominantly in the medial temporal lobe in the total sample, keeping with prior studies, and there was a trend towards a similar localization in both age groups.^{41,49,50,52,70} We suspect neurodegeneration in the medial temporal lobe was not significantly correlated with episodic memory performance due to methodological considerations, as there is relatively lower metabolic activity and more narrow dynamic range in the medial temporal lobe on FDG-PET in normal ageing.⁸⁸ It is also possible there is an FDG-PET hypometabolism floor effect in this region in patients with symptomatic Alzheimer’s disease. Semantic memory localization in the left-predominant temporal and inferior frontal cortices aligned with prior functional imaging.^{89–91} Language performance correlated with tau and neurodegeneration in a left-predominant perisylvian distribution along known language circuitry. Executive dysfunction associated with tau and neurodegeneration in regions seen in prior studies^{41,47} that overlap with the dorsal attention and frontoparietal executive control networks (and include posterior brain regions).^{92–94} Visuospatial function correlated with tau and neurodegeneration in the right greater than left occipital and posterior parietal lobes, conforming with prior spatial independent component analyses for visual functioning in Alzheimer’s disease and the posterior subtype identified in network-based models of tau spread.^{95,96} This aligns with prior *in vivo*^{36,38,41,47,49,50} and neuropathological evidence^{77,81} that the

location of neurofibrillary tangles appears to localize with cognitive domain deficits in Alzheimer's disease.

Tau in the right occipital cortex appeared to have a stronger correlation with visuospatial performance in LOAD compared to EOAD. It is possible that visuospatial performance is more closely associated with focal occipital tau in LOAD, and with more diffuse cortical tau in EOAD. This aligns with recently proposed tau-based subtypes of Alzheimer's disease, where similar visuospatial impairment was seen in both the posterior subtype (associated with an older onset age and early occipital tau) and in the medial temporal lobe-sparing subtype (associated with a younger onset age and early parietal tau).⁹⁶ With the exception of visuospatial performance, we overall found no meaningful or consistent differences in the correlation between tau and cognitive performance between age groups. Prior studies found an association between tau and cognition in patients with atypical Alzheimer's disease^{49,97} and with LOAD.^{50,79,98–100} Our results extend this by illustrating the correlation between tau and domain-specific cognition in a relatively larger sample of patients with EOAD. Additionally, our results suggest that the correlation appears similar between age groups, despite potential heterogeneity in the burden of tau and other neurodegeneration-related protein aggregates with age.^{8,55}

Neurodegeneration as measured by FDG-PET was significantly correlated and topographically aligned with cognitive performance in the total sample and both age groups. Compared to tau, hypometabolism appeared to be more spatially restricted but to also have a stronger correlation with cognitive performance. This may be due to neurodegeneration being a downstream event in the pathogenesis of Alzheimer's disease, closer to the onset of symptoms compared to amyloid and tau accumulation. A recent study also found that the spatial pattern of significant association between FTP-PET binding and cognition was more widespread than the association between cortical thickness on MRI (another biomarker of neurodegeneration) and cognition.⁵⁰ Alternatively, we cannot rule out that these differences between neurodegeneration and tau are statistically driven. FDG-PET was only available in 74% of participants who had FTP-PET, creating a higher threshold on voxel-wise analyses necessary to reach statistical significance.

In light of these results, age-related differences in clinical severity in the Alzheimer's disease spectrum may instead be due to greater neurofibrillary tangle burden, faster tau accumulation,⁵² or differing biochemical features of tau in younger patients.⁵⁵ There may also be a role of selection bias where older patients with a greater burden of tau may be too impaired for participation in research studies given potentially lower brain reserve and increased likelihood of co-pathologies.¹² Additionally, the increased frequency of non-amnesic symptoms in younger patients may be attributed to a different localization of tau pathology,³⁶ as younger patients have more cortical-predominant tau.^{96,101} This may be due to differences in underlying selective network vulnerability in younger patients, which may even be neurodevelopmental, as prior mathematical and visuospatial learning disabilities have been associated with PCA and language learning disabilities with lvPPA.^{49,95,102–104} This is also supported by recent studies showing those with non-amnesic symptoms have a neocortical origin of disease and that tau subsequently spreads systematically through distinct networks.^{96,105,106}

In mediation analyses, tau had an association with executive function independent of neurodegeneration in all age groups, with language in EOAD and in the total sample and with visuospatial function in the total sample. Neurodegeneration mediated the association between tau and cognition in all domains except episodic memory in LOAD. Tau has been demonstrated to have

an association with cognition independent of neurodegeneration in multiple prior studies.^{41,47,50,107} Our study extends prior evidence from atrophy-based biomarkers of neurodegeneration by showing the results are similar when evaluating local relationships using FDG-PET and within both EOAD and LOAD groups.^{47,50,107} Previous studies have observed that FTP-PET is more strongly associated with FDG-PET hypometabolism than with atrophy.^{38,51} The authors speculate this may be due to FDG-PET being more sensitive to the effects of tau or due to PET imaging modalities being more methodologically consistent than comparisons between PET and MRI.^{38,51} One possible explanation for tau neurotoxicity is recent evidence that tau independently induces cerebrovascular dysfunction by suppressing neurovascular coupling.¹⁰⁸ This has also been demonstrated in neuroimaging studies showing that reduced relative cerebral blood flow is associated with tau and cognition in Alzheimer's disease.^{41,109} A second possible explanation is that tau affects cognition before neurodegeneration occurs.¹⁰⁷ Tau may lead to impaired neuronal transmission¹¹⁰ and brain network dysfunction^{95,111} prior to neurodegeneration. This would conform with recent longitudinal evidence that tau is associated with future cortical atrophy measures of neurodegeneration,⁵³ cognitive decline⁵² and clinical progression.^{100,112}

A strength of the present study is that it includes a larger and more heterogeneous sample of symptomatic Alzheimer's disease patients compared to prior studies. Additionally, it is the first direct voxel-wise comparison between age groups of clinical-PET correlations to our knowledge. The results were similar across the heterogeneous sample, even when excluding atypical Alzheimer's disease variants, supporting internal validity and suggesting that tau is similarly correlated with cognitive performance across the heterogeneity of Alzheimer's disease phenotypes and ages. An additional strength is the use of multimodal PET imaging to capture key molecular pathology and neurodegeneration measures in the Alzheimer's disease pathophysiological cascade. The present study has limitations. First, we may have been underpowered to detect more subtle interactions between age groups and PET impacting associations with cognition. While ours is the largest multimodal PET study thus far exploring this question in EOAD to our knowledge, this question should be further evaluated in future larger studies. Second, these patients were recruited to an expert tertiary care centre, which creates selection bias as the proportion of patients with non-amnesic symptoms in both age groups is not generalizable to the population. Additionally, there was a lack of racial and ethnic diversity and participants were highly educated in the sample. Third, FDG-PET was available for most but not all patients, limiting our ability to directly compare multimodal PET biomarkers. Fourth, mediation analyses were limited to evaluating local relationships and did not account for possible distant relationships between FTP-PET, FDG-PET and domain-specific cognitive performance. As a cross-sectional observational study, this study was unable to assess causal relationships or longitudinal progression.

In conclusion, both tau and neurodegeneration appear to similarly localize and correlate with cognitive symptoms in EOAD and LOAD. These results provide additional support for including patients with EOAD in Alzheimer's disease studies given the similar association between pathology and cognitive performance across age groups. The results also support tau PET as a biomarker that captures molecular pathology specific to Alzheimer's disease and correlates with cognitive performance across the broad spectrum of ages and clinical phenotypes in Alzheimer's disease.

Acknowledgements

We would like to thank Dr William Jagust and his team for performing PET scans and Karen Smith for her efforts in coordinating the data collection. Avid Radiopharmaceuticals enabled the use of the FTP-PET tracer, but did not provide direct funding and were not involved in data analysis or interpretation.

Funding

Funding sources include: National Institute on Aging Grants P30-AG062422 (Alzheimer's Disease Research Center, B.L.M., H.J.R., G.D.R.), P01-AG019724 (Project Program Grant; B.L.M., H.J.R., G.D.R.), R35-AG072362 (G.D.R. and K.P.), K99 AG065501 (R.L.J.), R01 AG045611 (G.D.R.), Alzheimer's Association AACSF-19-617663 (D.N.S.), Rainwater Charitable Foundation (G.D.R.), a gift from Edward and Pearl Fein (G.D.R.), Race Against Dementia Alzheimer's Research UK ARUK-RADF2021A-010 (M.M.), the Cambridge University Centre for Parkinson-Plus RG95450 and the National Institute for Health Research (NIHR) Cambridge Biomedical Research Centre BRC-1215-20014 (M.M., the views expressed are those of the authors and not necessarily those of the NIHR or the Department of Health and Social Care).

Competing interests

B.L.M. receives research support from the NIH/NIA and the Centers for Medicare & Medicaid Services (CMS) as grants for the Memory and Aging Center. As an additional disclosure, B.L.M. serves as Medical Director for the John Douglas French Foundation; Scientific Director for the Tau Consortium; Director/Medical Advisory Board of the Larry L. Hillblom Foundation; Scientific Advisory Board Member for the National Institute for Health Research Cambridge Biomedical Research Centre and its subunit, the Biomedical Research Unit in Dementia (UK); and Board Member for the American Brain Foundation (ABF). R.L.J. serves as an Associate Editor for Alzheimer's Research & Therapy. G.D.R. has research support from Avid Radiopharmaceuticals, GE Healthcare, Life Molecular Imaging, Genentech; has served as a consultant for Eisai, Eli Lilly, Genentech, GE Healthcare, Johnson & Johnson, Roche; and serves as an Associate Editor for *JAMA Neurology*. All other authors report no competing interests.

Supplementary material

Supplementary material is available at *Brain* online.

References

- Vieira RT, Caixeta L, Machado S, et al. Epidemiology of early-onset dementia: A review of the literature. *Clin Pract Epidemiol Ment Health*. 2013;9:88–95.
- Lambert MA, Bickel H, Prince M, et al. Estimating the burden of early onset dementia; Systematic review of disease prevalence. *Eur J Neurol*. 2014;21:563–569.
- Zhu XC, Tan L, Wang HF, et al. Rate of early onset Alzheimer's disease: A systematic review and meta-analysis. *Ann Transl Med*. 2015;3:38.
- Cacace R, Sleegers K, Van Broeckhoven C. Molecular genetics of early-onset Alzheimer's disease revisited. *Alzheimers Dement*. 2016;12:733–748.
- Jarmolowicz AI, Chen HY, Panegyres PK. The patterns of inheritance in early-onset dementia: Alzheimer's disease and frontotemporal dementia. *Am J Alzheimers Dis Other Demen*. 2015;30:299–306.
- Campion D, Dumanchin C, Hannequin D, et al. Early-onset autosomal dominant Alzheimer disease: prevalence, genetic heterogeneity, and mutation spectrum. *Am J Hum Genet*. 1999;65:664–670.
- Ho GJ, Hansen LA, Alford MF, et al. Age at onset is associated with disease severity in Lewy body variant and Alzheimer's disease. *Neuroreport*. 2002;13:1825–1828.
- Marshall GA, Fairbanks LA, Tekin S, Vinters HV, Cummings JL. Early-onset Alzheimer's disease is associated with greater pathologic burden. *J Geriatr Psychiatry Neurol*. 2007;20:29–33.
- Savva GM, Wharton SB, Ince PG, et al. Age, neuropathology, and dementia. *N Engl J Med*. 2009;360:2302–2309.
- Davidson YS, Raby S, Foulds PG, et al. TDP-43 pathological changes in early onset familial and sporadic Alzheimer's disease, late onset Alzheimer's disease and Down's syndrome: Association with age, hippocampal sclerosis and clinical phenotype. *Acta Neuropathol*. 2011;122:703–713.
- Robinson JL, Lee EB, Xie SX, et al. Neurodegenerative disease concomitant proteinopathies are prevalent, age-related and APOE4-associated. *Brain*. 2018;141:2181–2193.
- Spina S, La Joie R, Petersen C, et al. Comorbid neuropathological diagnoses in early versus late-onset Alzheimer's disease. *Brain*. 2021;144:2186–2198.
- Lawlor BA, Ryan TM, Schmeidler J, Mohs RC, Davis KL. Clinical symptoms associated with age at onset in Alzheimer's disease. *The American Journal of Psychiatry*. 1994;151:1646–1649.
- Smits LL, Pijnenburg YAL, Koedam ELGE, et al. Early onset Alzheimer's disease is associated with a distinct neuropsychological profile. *J Alzheimers Dis*. 2012;30:101–108.
- Palasí A, Gutiérrez-Iglesias B, Alegret M, et al. Differentiated clinical presentation of early and late-onset Alzheimer's disease: Is 65 years of age providing a reliable threshold? *J Neurol*. 2015;262:1238–1246.
- Joubert S, Gour N, Guedj E, et al. Early-onset and late-onset Alzheimer's disease are associated with distinct patterns of memory impairment. *Cortex*. 2016;74:217–232.
- Mendez MF. Early-onset Alzheimer's disease. *Neurol Clin*. 2017; 35:263–281.
- Mendez MF. The accurate diagnosis of early-onset dementia. *Int J Psychiatry Med*. 2006;36:401–412.
- Bentham P, La Fontaine J. Services for younger people with dementia. *Psychiatry*. 2005;4:100–103.
- Werner P, Stein-Shvachman I, Korczyn AD. Early onset dementia: Clinical and social aspects. *Int Psychogeriatr*. 2009;21:631–636.
- Wattmo C, Wallin ÅK. Early- versus late-onset Alzheimer's disease in clinical practice: Cognitive and global outcomes over 3 years. *Alzheimers Res Ther*. 2017;9:70.
- Jacobs D, Sano M, Marder K, et al. Age at onset of Alzheimer's disease: Relation to pattern of cognitive dysfunction and rate of decline. *Neurology*. 1994;44:1215–1220.
- Chang KJ, Hong CH, Lee KS, et al. Mortality risk after diagnosis of early-onset Alzheimer's disease versus late-onset Alzheimer's disease: A propensity score matching analysis. *J Alzheimers Dis*. 2017;56:1341–1348.
- Klunk WE, Engler H, Nordberg A, et al. Imaging brain amyloid in Alzheimer's disease with Pittsburgh compound-B. *Ann Neurol*. 2004;55:306–319.
- Driscoll I, Troncoso JC, Rudow G, et al. Correspondence between in vivo 11C-PiB-PET amyloid imaging and postmortem, region-matched assessment of plaques. *Acta Neuropathol*. 2012;124:823–831.

26. La Joie R, Ayakta N, Seeley WW, et al. Multisite study of the relationships between antemortem [¹¹C]PIB-PET centiloid values and postmortem measures of Alzheimer's disease neuropathology. *Alzheimers Dement*. 2019;15:205–216.
27. Cho H, Seo SW, Kim JH, et al. Amyloid deposition in early onset versus late onset Alzheimer's disease. *J Alzheimers Dis*. 2013;35:813–821.
28. Ossenkoppele R, Zwan MD, Tolboom N, et al. Amyloid burden and metabolic function in early-onset Alzheimer's disease: Parietal lobe involvement. *Brain*. 2012;135(Pt 7):2115–2125.
29. Rabinovici GD, Furst AJ, Alkalay A, et al. Increased metabolic vulnerability in early-onset Alzheimer's disease is not related to amyloid burden. *Brain*. 2010;133(Pt 2):512–528.
30. Scholl M, Lockhart SN, Schonhaut DR, et al. PET Imaging of tau deposition in the aging human brain. *Neuron*. 2016;89:971–982.
31. La Joie R, Visani AV, Lesman-Segev OH, et al. Association of APOE4 and clinical variability in Alzheimer disease with the pattern of tau- and amyloid-PET. *Neurology*. 2021;96:e650–e661.
32. Xia CF, Arteaga J, Chen G, et al. [¹⁸F]T807, a novel tau positron emission tomography imaging agent for Alzheimer's disease. *Alzheimers Dement*. 2013;9:666–676.
33. Chien DT, Bahri S, Szardenings AK, et al. Early clinical PET imaging results with the novel PHF-tau radioligand [F-18]-T807. *J Alzheimers Dis*. 2013;34:457–468.
34. Marquié M, Normandin MD, Vanderburg CR, et al. Validating novel tau positron emission tomography tracer [F-18]-AV-1451 (T807) on postmortem brain tissue. *Ann Neurol*. 2015;78:787–800.
35. Fleisher AS, Pontecorvo MJ, Devous MD, et al. Positron emission tomography imaging with [¹⁸F]flortaucipir and postmortem assessment of Alzheimer disease neuropathologic changes. *JAMA Neurol*. 2020;77:829–839.
36. Ossenkoppele R, Schonhaut DR, Scholl M, et al. Tau PET patterns mirror clinical and neuroanatomical variability in Alzheimer's disease. *Brain*. 2016;139(Pt 5):1551–1567.
37. Schöll M, Ossenkoppele R, Strandberg O, et al. Distinct 18F-AV-1451 tau PET retention patterns in early- and late-onset Alzheimer's disease. *Brain*. 2017;140:2286–2294.
38. Whitwell JL, Graff-Radford J, Tosakulwong N, et al. Imaging correlations of tau, amyloid, metabolism, and atrophy in typical and atypical Alzheimer's disease. *Alzheimers Dement*. 2018;14:1005–1014.
39. Iaccarino L, La Joie R, Edwards L, et al. Spatial relationships between molecular pathology and neurodegeneration in the Alzheimer's disease continuum. *Cereb Cortex*. 2021;31:1–14.
40. Josephs KA, Tosakulwong N, Graff-Radford J, et al. MRI And flortaucipir relationships in Alzheimer's phenotypes are heterogeneous. *Ann Clin Transl Neurol*. 2020;7:707–721.
41. Visser D, Wolters EE, Verfaillie SCJ, et al. Tau pathology and relative cerebral blood flow are independently associated with cognition in Alzheimer's disease. *Eur J Nucl Med Mol Imaging*. 2020;47:3165–3175.
42. Kato T, Inui Y, Nakamura A, Ito K. Brain fluorodeoxyglucose (FDG) PET in dementia. *Ageing Res Rev*. 2016;30:73–84.
43. Kim EJ, Cho SS, Jeong Y, et al. Glucose metabolism in early onset versus late onset Alzheimer's disease: An SPM analysis of 120 patients. *Brain*. 2005;128(Pt 8):1790–1801.
44. Aziz AL, Giusiano B, Joubert S, et al. Difference in imaging biomarkers of neurodegeneration between early and late-onset amnesic Alzheimer's disease. *Neurobiol Aging*. 2017;54:22–30.
45. Lehmann M, Ghosh PM, Madison C, et al. Diverging patterns of amyloid deposition and hypometabolism in clinical variants of probable Alzheimer's disease. *Brain*. 2013;136:844–858.
46. Koychev I, Gunn RN, Firouzian A, et al. PET Tau and amyloid- β burden in mild Alzheimer's disease: Divergent relationship with age, cognition, and cerebrospinal fluid biomarkers. *J Alzheimers Dis*. 2017;60:283–293.
47. Bejanin A, Schonhaut DR, La Joie R, et al. Tau pathology and neurodegeneration contribute to cognitive impairment in Alzheimer's disease. *Brain*. 2017;140:3286–3300.
48. Pontecorvo MJ, Devous MD, Navitsky M, et al. Relationships between flortaucipir PET tau binding and amyloid burden, clinical diagnosis, age and cognition. *Brain*. 2017;140:748–763.
49. Phillips JS, Das SR, McMillan CT, et al. Tau PET imaging predicts cognition in atypical variants of Alzheimer's disease. *Hum Brain Mapp*. 2018;39:691–708.
50. Digma LA, Madsen JR, Reas ET, et al. Tau and atrophy: Domain-specific relationships with cognition. *Alzheimers Res Ther*. 2019;11:65.
51. Sintini I, Schwarz CG, Martin PR, et al. Regional multimodal relationships between tau, hypometabolism, atrophy, and fractional anisotropy in atypical Alzheimer's disease. *Hum Brain Mapp*. 2019;40:1618–1631.
52. Jack CR, Wiste HJ, Weigand SD, et al. Predicting future rates of tau accumulation on PET. *Brain*. 2020;143:3136–3150.
53. La Joie R, Visani AV, Baker SL, et al. Prospective longitudinal atrophy in Alzheimer's disease correlates with the intensity and topography of baseline tau-PET. *Sci Transl Med*. 2020;12:eaa5732. doi:10.1126/scitranslmed.aau5732
54. Boon BDC, Bulk M, Jonker AJ, et al. The coarse-grained plaque: a divergent $\text{a}\beta$ plaque-type in early-onset Alzheimer's disease. *Acta Neuropathol*. 2020;140:811–830.
55. Dujardin S, Commins C, Lathuiliere A, et al. Tau molecular diversity contributes to clinical heterogeneity in Alzheimer's disease. *Nat Med*. 2020;26:1256–1263.
56. Ossenkoppele R, Lyoo CH, Jester-Broms J, et al. Assessment of demographic, genetic, and imaging variables associated with brain resilience and cognitive resilience to pathological tau in patients with Alzheimer disease. *JAMA Neurol*. 2020;77:632–642.
57. McKhann GM, Knopman DS, Chertkow H, et al. The diagnosis of dementia due to Alzheimer's disease: recommendations from the National Institute on Aging–Alzheimer's Association workgroups on diagnostic guidelines for Alzheimer's disease. *Alzheimers Dement*. 2011;7:263–269.
58. Albert MS, DeKosky ST, Dickson D, et al. The diagnosis of mild cognitive impairment due to Alzheimer's disease: recommendations from the National Institute on Aging–Alzheimer's Association workgroups on diagnostic guidelines for Alzheimer's disease. *Alzheimers Dement*. 2011;7:270–279.
59. Montenegro PH, Baugh CM, Daneshvar DH, et al. Clinical subtypes of chronic traumatic encephalopathy: Literature review and proposed research diagnostic criteria for traumatic encephalopathy syndrome. *Alzheimers Res Ther*. 2014;6:68.
60. Crutch SJ, Schott JM, Rabinovici GD, et al. Consensus classification of posterior cortical atrophy. *Alzheimers Dement*. 2017;13:870–884.
61. Gorno-Tempini ML, Hillis AE, Weintraub S, et al. Classification of primary progressive aphasia and its variants. *Neurology*. 2011;76:1006–1014.
62. Kramer JH, Jurik J, Sha SJ, et al. Distinctive neuropsychological patterns in frontotemporal dementia, semantic dementia, and Alzheimer disease. *Cogn Behav Neurol*. 2003;16:211–218.
63. Strom A, Iaccarino L, Edwards L, et al. Cortical hypometabolism reflects local atrophy and tau pathology in symptomatic Alzheimer's disease. *Brain*. 2021;145:713–728.

64. Knopman D, Weintraub S, Pankratz V. Language and behavior domains enhance the value of the clinical dementia rating scale. *Alzheimers Dement*. 2011;7:293–299.
65. Nys GMS, van Zandvoort MJE, de Kort PLM, Jansen BPW, Kappelle LJ, de Haan EHF. Restrictions of the Mini-Mental State Examination in acute stroke. *Arch Clin Neuropsychol*. 2005;20:623–629.
66. Villeneuve S, Rabinovici GD, Cohn-Sheehy BI, et al. Existing Pittsburgh compound-B positron emission tomography thresholds are too high: Statistical and pathological evaluation. *Brain*. 2015;138(Pt 7):2020–2033.
67. Lesman-Segev OH, La Joie R, Stephens ML, et al. Tau PET and multimodal brain imaging in patients at risk for chronic traumatic encephalopathy. *Neuroimage Clin*. 2019;24:102025.
68. Jack CR, Wiste HJ, Weigand SD, et al. Defining imaging biomarker cut points for brain aging and Alzheimer's disease. *Alzheimers Dement*. 2017;13:205–216.
69. Baker SL, Maass A, Jagust WJ. Considerations and code for partial volume correcting [18F]-AV-1451 tau PET data. *Data Brief*. 2017;15:648–657.
70. Maass A, Landau S, Baker SL, et al. Comparison of multiple tau-PET measures as biomarkers in aging and Alzheimer's disease. *Neuroimage*. 2017;157:448–463.
71. Müller-Gärtner HW, Links JM, Prince JL, et al. Measurement of radiotracer concentration in brain gray matter using positron emission tomography: MRI-based correction for partial volume effects. *J Cereb Blood Flow Metab*. 1992;12:571–583.
72. MATLAB. Version 8.5.0.197613(R2015a). The MathWorks Inc.; 2015.
73. Xia M, Wang J, He Y. Brainnet viewer: A network visualization tool for human brain connectomics. *PLoS One*. 2013;8:e68910.
74. Wickham H. *Ggplot2: Elegant graphics for data analysis*. Springer-Verlag New York; 2009.
75. R Core Team. R: A Language and Environment for Statistical Computing. R Foundation for Statistical Computing; 2017. <https://www.R-project.org/>.
76. Tingley D, Yamamoto T, Hirose K, Keele L, Imai K. Mediation: R package for causal mediation analysis. *J Stat Softw*. 2014;59:1–38.
77. Petersen C, Nolan AL, de Paula França Resende E, et al. Alzheimer's disease clinical variants show distinct regional patterns of neurofibrillary tangle accumulation. *Acta Neuropathol*. 2019;138:597–612.
78. Furst AJ, Rabinovici GD, Rostomian AH, et al. Cognition, glucose metabolism and amyloid burden in Alzheimer's disease. *Neurobiol Aging*. 2012;33:215–225.
79. Ossenkoppele R, Smith R, Ohlsson T, et al. Associations between tau, a β , and cortical thickness with cognition in Alzheimer disease. *Neurology*. 2019;92:e601–e612.
80. Giannakopoulos P, Herrmann FR, Bussière T, et al. Tangle and neuron numbers, but not amyloid load, predict cognitive status in Alzheimer's disease. *Neurology*. 2003;60:1495–1500.
81. Nelson PT, Alafuzoff I, Bigio EH, et al. Correlation of Alzheimer disease neuropathologic changes with cognitive status: A review of the literature. *J Neuropathol Exp Neurol*. 2012;71:362–381.
82. Villemagne VL, Burnham S, Bourgeat P, et al. Amyloid β deposition, neurodegeneration, and cognitive decline in sporadic Alzheimer's disease: A prospective cohort study. *Lancet Neurol*. 2013;12:357–367.
83. Mintun MA, Lo AC, Duggan Evans C, et al. Donanemab in early Alzheimer's disease. *N Engl J Med*. 2021;384:1691–1704.
84. Viola KL, Klein WL. Amyloid β oligomers in Alzheimer's disease pathogenesis, treatment, and diagnosis. *Acta Neuropathol*. 2015;129:183–206.
85. Santos AN, Ewers M, Minthon L, et al. Amyloid- β oligomers in cerebrospinal fluid are associated with cognitive decline in patients with Alzheimer's disease. *J Alzheimers Dis*. 2012;29:171–176.
86. Jongbloed W, Bruggink KA, Kester MI, et al. Amyloid- β oligomers relate to cognitive decline in Alzheimer's disease. *J Alzheimers Dis*. 2015;45:35–43.
87. Meng X, Li T, Wang X, et al. Association between increased levels of amyloid- β oligomers in plasma and episodic memory loss in Alzheimer's disease. *Alzheimers Res Ther*. 2019;11:89.
88. Berti V, Mosconi L, Pupi A. Brain: normal variations and benign findings in fluorodeoxyglucose-PET/computed tomography imaging. *PET Clin*. 2014;9:129–140.
89. Posner MI, Petersen SE, Fox PT, Raichle ME. Localization of cognitive operations in the human brain. *Science*. 1988;240:1627–1631.
90. Chertkow H, Whatmough C, Saumier D, Duong A. Cognitive neuroscience studies of semantic memory in Alzheimer's disease. *Prog Brain Res*. 2008;169:393–407.
91. Peelle JE, Powers J, Cook PA, Smith EE, Grossman M. Frontotemporal neural systems supporting semantic processing in Alzheimer's disease. *Cogn Affect Behav Neurosci*. 2014;14:37–48.
92. Yeo BTT, Krienen FM, Sepulcre J, et al. The organization of the human cerebral cortex estimated by intrinsic functional connectivity. *J Neurophysiol*. 2011;106:1125–1165.
93. Hansson O, Grothe MJ, Strandberg TO, et al. Tau pathology distribution in Alzheimer's disease corresponds differentially to cognition-relevant functional brain networks. *Front Neurosci*. 2017;11:167.
94. Vincent JL, Kahn I, Snyder AZ, Raichle ME, Buckner RL. Evidence for a frontoparietal control system revealed by intrinsic functional connectivity. *J Neurophysiol*. 2008;100:3328–3342.
95. Jones DT, Knopman DS, Gunter JL, et al. Cascading network failure across the Alzheimer's disease spectrum. *Brain*. 2016;139(Pt 2):547–562.
96. Vogel JW, Young AL, Oxtoby NP, et al. Four distinct trajectories of tau deposition identified in Alzheimer's disease. *Nat Med*. 2021;27:871–881.
97. Xia C, Makarets SJ, Caso C, et al. Association of in vivo [18F] AV-1451 tau PET imaging results with cortical atrophy and symptoms in typical and atypical Alzheimer disease. *JAMA Neurol*. 2017;74:427–436.
98. Brier MR, Gordon B, Friedrichsen K, et al. Tau and a β imaging, CSF measures, and cognition in Alzheimer's disease. *Sci Transl Med*. 2016;8:338ra66.
99. Maass A, Lockhart SN, Harrison TM, et al. Entorhinal tau pathology, episodic memory decline, and neurodegeneration in aging. *J Neurosci*. 2018;38:530–543.
100. Hanseeuw BJ, Betensky RA, Jacobs HIL, et al. Association of amyloid and tau with cognition in preclinical Alzheimer disease. *JAMA Neurol*. 2019;76:915–924.
101. Murray ME, Graff-Radford NR, Ross OA, Petersen RC, Duara R, Dickson DW. Neuropathologically defined subtypes of Alzheimer's disease with distinct clinical characteristics: a retrospective study. *Lancet Neurol*. 2011;10:785–796.
102. Miller ZA, Mandelli ML, Rankin KP, et al. Handedness and language learning disability differentially distribute in progressive aphasia variants. *Brain*. 2013;136(Pt 11):3461–3473.
103. Miller ZA, Rosenberg L, Santos-Santos MA, et al. Prevalence of mathematical and visuospatial learning disabilities in patients with posterior cortical atrophy. *JAMA Neurol*. 2018;75:728–737.

104. Franzmeier N, Dewenter A, Frontzkowski L, et al. Patient-centered connectivity-based prediction of tau pathology spread in Alzheimer's disease. *Sci Adv.* 2020;6:eabd1327. doi:10.1126/sciadv.abd1327
105. Phillips JS, Da Re F, Dratch L, et al. Neocortical origin and progression of gray matter atrophy in nonamnesic Alzheimer's disease. *Neurobiol Aging.* 2018;63:75–87.
106. Vogel JW, Iturria-Medina Y, Strandberg OT, et al. Spread of pathological tau proteins through communicating neurons in human Alzheimer's disease. *Nat Commun.* 2020;11:2612.
107. Mattsson N, Insel PS, Donohue M, et al. Predicting diagnosis and cognition with 18F-AV-1451 tau PET and structural MRI in Alzheimer's disease. *Alzheimers Dement.* 2019;15:570–580.
108. Park L, Hochrainer K, Hattori Y, et al. Tau induces PSD95-neuronal NOS uncoupling and neurovascular dysfunction independent of neurodegeneration. *Nat Neurosci.* 2020;23:1079–1089.
109. Albrecht D, Isenberg AL, Stradford J, et al. Associations between vascular function and tau PET are associated with global cognition and amyloid. *J Neurosci.* 2020;40:8573–8586.
110. Menkes-Caspi N, Yamin HG, Kellner V, Spires-Jones TL, Cohen D, Stern EA. Pathological tau disrupts ongoing network activity. *Neuron.* 2015;85:959–966.
111. Jones DT, Graff-Radford J, Lowe VJ, et al. Tau, amyloid, and cascading network failure across the Alzheimer's disease spectrum. *Cortex.* 2017;97:143–159.
112. Cho H, Choi JY, Lee HS, et al. Progressive tau accumulation in Alzheimer disease: 2-year follow-up study. *J Nucl Med.* 2019;60:1611–1621.